Mesonic X-Rays from Capture of Cosmic-Ray μ Mesons in a Chemical Compound*†

A. FAFARMAN‡ AND M. H. SHAMOS
Department of Physics, New York University, Washington Square College, New York, New York
(Received June 7, 1955)

Measurements have been made of the x-rays emitted by mesonic carbon and oxygen atoms formed by the capture of negative cosmic ray μ mesons. A 4-liter tank of liquid scintillator, dioxane, $C_4O_2H_8$ (plus 10 g/l of *p*-terphenyl) served as the absorber and as the detector for the stopping of cosmic-ray μ mesons. The mesons were identified by the method of delayed coincidences. The mesonic x-rays from the dioxane were detected by a scintillation spectrometer. Spectrometer pulses in coincidence with the stopping meson were lengthened and their pulse height recorded on a recording milliammeter. The time distribution of the delayed coincidences was recorded over the delay interval 0.5 to 8.0 μsec. The measured $2p-1s$ transition energies of 82 kev and 145 kev, for carbon and oxygen respectively, agree with the simple Bohr orbit calculations within the precision of the measurement. The observed ratio of captures by oxygen and carbon (0.33 ± 0.04) does not agree with the Z-dependence predicted by Fermi and Teller for mesonic atom formation by chemical compounds (0.67) nor with the simple stopping power calculation (0.50); however, in view of the thick absorber (14 cm depth of dioxane), the above experimental ratio is uncertain because of Compton degradation of the oxygen $2p-1s$ radiation which shifts some events from the oxygen to the carbon peak. The observed distribution of delays is consistent with the assignment of the observed radiation to μ-meson capture.

I. INTRODUCTION

FOLLOWING the suggestions of Wheeler[1,2] on the applications of the negative μ meson as a probe for nuclear electric and magnetic fields, the spectroscopy of μ mesonic atoms has been applied to several problems. Fitch and Rainwater[3] have made accurate determinations of nuclear radii in absorbers of high Z. Conversely, by using materials of low Z, and the precisely known K x-ray absorption edges of absorbing foils, several investigators[4,5] have determined the μ-meson mass with high precision, permitting a comparison with the mass obtained by other methods.[6]

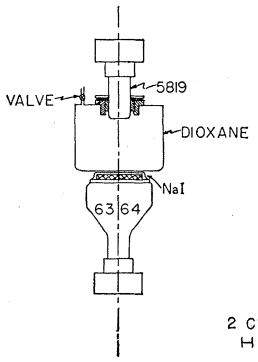

FIG. 1. Apparatus for the study of the capture of negative μ mesons in carbon and oxygen. A 5819 photomultiplier views the tank of dioxane (or toluene) scintillator in which the stopping mesons are detected by the method of delayed coincidences. Mesonic x-rays are detected by a coincidence scintillation spectrometer which includes the NaI crystal and the 6364 photomultiplier; (the photomultipliers are attached to their respective preamplifiers; apparatus supports and photomultiplier mu metal shields are not shown).

However, the slowing down and capture of the negative μ meson into a mesonic Bohr orbit requires further study. For example, the present experimental evidence does not establish clearly the Z-dependence predicted by Fermi and Teller[7] for the relative number of captures on different elements of a chemical compound. The present experiment was intended to study this and related aspects of μ-meson capture by spectroscopy of the mesonic x-rays.

II. EXPERIMENTAL METHOD[8]

For low Z materials, e.g., carbon and oxygen, in which the life of the negative μ meson is not shortened appreciably, it was possible to study the mesonic x-rays with essentially no background and with no contribution from nuclear absorption gamma radiation or from (decay beta particle) bremsstrahlung. A large volume organic liquid scintillator was used as the absorber and as the detector for the stopping of μ

* Assisted in part by the U. S. Atomic Energy Commission and by the Office of Naval Research.
† A brief description of this research has been given at the 1955 Washington meeting of the American Physical Society [Phys. Rev. **99**, 623(A) (1955)].
‡ Submitted by A. Fafarman in partial fulfillment of the requirements for the degree of Doctor of Philosophy in the Graduate School of Arts and Science at New York University.
[1] J. A. Wheeler, Revs. Modern Phys. **21**, 133 (1949).
[2] J. A. Wheeler, Phys. Rev. **92**, 812 (1953).
[3] V. L. Fitch and J. Rainwater, Phys. Rev. **92**, 789 (1953). These measurements hold forth the possibility of resolving the $2p_{\frac{1}{2}}-2p_{\frac{3}{2}}$ to ground-state doublet of the Pb mesonic atom.
[4] Koslov, Fitch, and Rainwater, Phys. Rev. **95**, 291 (1954).
[5] S. DeBenedetti *et al.*, Phys. Rev. **94**, 766(A) (1954).
[6] Hydrogen constitutes a special case; see R. E. Marshak, *Meson Physics* (McGraw-Hill Book Company, Inc., New York, 1952), pp. 171, 172.
[7] E. Fermi and E. Teller, Phys. Rev. **72**, 399 (1947).
[8] Some earlier experiments on Pb mesonic atoms were performed in this laboratory using a different experimental method than that described above. [A. Fafarman and M. H. Shamos, Phys. Rev. **87**, 219(A) (1952)]. These experiments are summarized here. A conventional coincidence-anticoincidence GM counter telescope was used to select cosmic-ray mesons stopping in a Pb absorber. Gamma radiation coincident in time with the stopped meson ($\mu\gamma$ coincidence) was detected by a scintillation spectrometer which was placed outside of the direct meson beam and guarded by a double ring of anticoincidence GM counters. The measurements showed (continuous) gamma radiation of maximum energy 5.5 ± 1.5 Mev. The interpretation of the results was complicated by a high background. The rate of background events (Pb absorber removed) in the energy interval 1 to 10 Mev was 0.09 ± 0.03/hr, while the corresponding rate with the Pb absorber in place (foreground rate) was 0.25 ± 0.04/hr. The high background was due principally to photon secondaries of fast mesons and of decay positrons. The difference between the foreground and background included (in addition to the mesonic x-rays of Pb), the gamma radiation resulting from the nuclear absorption of the negative mesons and the bremsstrahlung of a fraction of the decay positrons which result from the decay of positive μ mesons in the absorber; (the resolving time for $\mu\gamma$ coincidences was 0.9 μsec and bremsstrahlung from positrons appearing within this interval could contribute to the foreground minus background rate).

mesons[9–11]; the μ mesons were identified by the method of delayed coincidences. The mesonic x-rays were detected by a NaI scintillation spectrometer in time coincidence with the stopped meson; i.e., the measurement was made of the energy of the associated *prompt* radiation without measuring radiation associated with the *delayed* meson decay beta particle or *delayed* nuclear radiation.

The apparatus for the measurement of the mesonic x-rays from carbon and oxygen consisted essentially of two scintillation detectors together with the associated electronics. The detectors are illustrated in Fig. 1. The upper detector was a 4-liter tank of liquid scintillator 19 cm in diameter $\times$14 cm high, viewed by a single 5819 photomultiplier. The tank was filled with toluene (plus 10 g/l *p*-terphenyl) or with dioxane (plus 10 g/l *p*-terphenyl) for measurements on carbon and on carbon plus oxygen respectively. The dioxane was comparable to toluene in scintillation efficiency[12] although some dioxane had to be dehydrated for satisfactory performance.[13] The tank was constructed from a thin-walled aluminum pot; the joints were sealed with Sauereisen No. 31 cement.[14]

A threaded ring was cemented to the 5819 tube and screwed into a threaded bushing on the tank, sealing against it by means of a corrugated lead gasket. A valve was used to vent the tank. Delayed coincidences in this tank (with a delay of 0.5 to 8.0 μsec) will be identified as μ-β events.

The gamma detector was a 4-in. diameter $\times$ $\frac{1}{2}$-in. thick sodium iodide crystal, hermetically sealed in a 0.025-in. wall aluminum container. The inner surface was a fired aluminum oxide coating of negligible absorption which served as a diffuse reflector to secure more uniform light collection in various parts of the crystal. A type 6364, 5-in. photomultiplier was used with the crystal; this combination gave a pulse height distribution curve for the Cs^{137} photopeak (663 kev) having a full width (at half-maximum) of 17%. Events occuring in this crystal will be identified as γ events.

Figure 2 is a block diagram of the electronics. The scintillation pulses are amplified in moderately fast amplifiers (rise time $1–2\times10^{-7}$ sec) and fed to a gated beam tube coincidence circuit. The width of the time resolution curve for the coincidence circuit is about 3×10^{-7} sec. A $\mu\gamma$ coincidence followed by a second pulse in the tank with a delay of 0.5 to 8.0 μsec (β pulse) is selected by the delay discriminator and sorted into one of four channels.

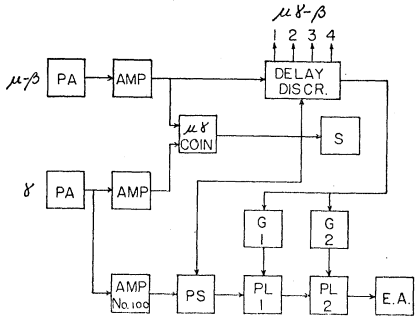

FIG. 2. Electronics for the study of negative μ meson capture. Pulses from the tank (μ-β) and from the NaI (γ) are amplified by preamplifiers, PA, and fast amplifiers, AMP. The γ pulse is amplified also in a slow amplifier, AMP No. 100; the pulse in this channel is stretched to 20 μsec by a pulse stretcher, PS, whenever a $\mu\gamma$ coincidence occurs. The stretched pulse is further lengthened by a doubly gated, G1G2, pulse lengthener, PL1 PL2, and recorded on an Esterline Angus recording milliammeter EA, only if the γ is accompanied by a delayed β event ($\mu\gamma$-β) as selected by the delay discriminator.

(1) $\mu\gamma$-β (delayed 0.5 to 2.5 μsec),
(2) $\mu\gamma$-β (delayed 2.5 to 4.4 μsec),
(3) $\mu\gamma$-β (delayed 4.4 to 6.3 μsec),
(4) $\mu\gamma$-β (delayed 6.3 to 8.0 μsec).

The delay discriminator furnishes a master pulse $(\mu\gamma\text{-}\beta)_{1234}$ whenever any of the four channels is actuated. The master pulse gates a two-stage pulse lengthener which lengthens the γ pulse to 2 seconds in duration and permits the amplitude of the γ pulse to be recorded on an Esterline Angus recording milliammeter.

The γ pulse which is used in the pulse height measurement is derived from the γ preamplifier, delay-line-shaped for a duration of 4 μsec and amplified with a rise time of 0.5 μsec and gain of 700 by a Los Alamos Model 100 amplifier. The pulse output of the amplifier is stretched to a duration of 20 μsec whenever a $\mu\gamma$ coincidence occurs, so that, if it proves to be a $\mu\gamma$-β event, the response of the pulse lengthener will be independent of the delay of the master output pulse from the delay discriminator.

III. CALIBRATION PROCEDURE

The following calibration procedure was used. Artificial pulses were supplied to the input of the preamplifier and plots of chart deflection, D', *vs* millivolts input were made (e.g., Fig. 3). The calibration pulse was a negative step signal with a 1000-μsec exponential decay (to minimize undershoot of the amplifier) and was generated by a Hg switch generator; the pulse amplitude was determined by a Helipot across a calibrated voltage source. Following this, a plot of the output pulse height, E, of the No. 100 amplifier *vs* millivolts input was made (see Fig. 3). The output pulse height in volts is measured by the E (voltage) setting of the differential discriminator which is used for

[9] F. D. S. Butement, Phil. Mag. **349**, 208 (1953).
[10] J. V. Jelley and W. J. Whitehouse, Proc. Phys. Soc. (London) **A66**, 454 (1953).
[11] C. L. Cowen *et al.*, Phys. Rev. **90**, 493 (1953).
[12] H. Kallmann (private communication).
[13] See L. F. Fieser, *Experiments in Organic Chemistry* (D. C. Heath, Boston, 1941), second edition, p. 368.
[14] Joints made with this cement were somewhat permeable for toluene and dioxane—aluminum welds should be used for permanent tanks.

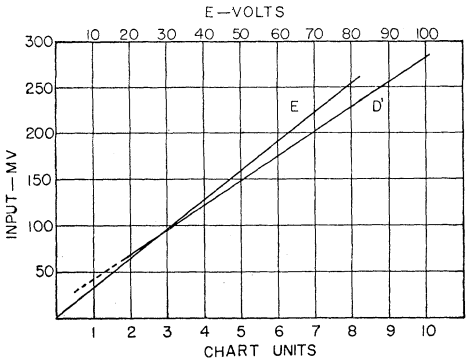

FIG. 3. Amplifier and pulse-lengthener calibrations. The ordinate is the amplitude in millivolts of the calibration pulse input. The abscissa (upper scale) gives the pulse output of the amplifier No. 100 as measured by the differential discriminator, E volts. The abscissa (lower scale) gives the chart deflection D'. The slight nonlinearity in the D' plot at small deflections is characteristic of diode pulse lengtheners.

analyzing the calibrating radioactive sources. The repetition rate of the Hg switch pulse generator is about 4/second in this part of the calibration, whereas single pulse operation is used for the chart deflection calibration.

The energy scale was determined by differential pulse-height analysis of the spectra of artificial radioactive sources (e.g., Figs. 4 and 5 for Cs^{137} and Ce^{144}).[15] Essentially the E (volts) scale of the differential discriminator served as the fiducial mark in these three calibrations, which had the end purpose of relating a particular chart deflection to a corresponding energy loss in the NaI crystal. The tank of scintillating liquid was removed during the calibrations.

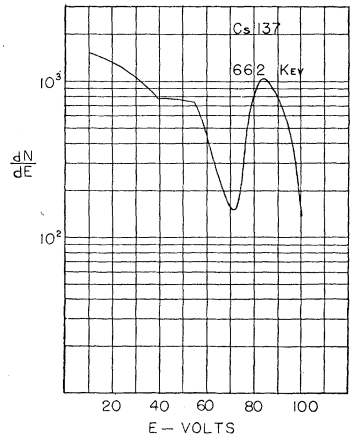

FIG. 4. Cs^{137} calibration curve. The ordinates are counts (per 20 seconds) for a 3 volt window; the abscissa is the pulse height in volts. The amplifier attenuation (Model 100 amplifier) is about 3 times the attenuation used for Fig. 5.

[15] The characteristic peaks in these spectra must be corrected by $-dE/2$ where dE is the differential discriminator window. This is seen easily by a graphical analysis for a differential discriminator which selects pulses in the voltage interval E to $(E-dE)$. The same analysis shows, incidentally, that the width of the pulse-height distribution curve is

$$\delta E/E \cong [(\delta E/E)_0^2 + (dE/E)^2]^{\frac{1}{2}},$$

where $(\delta E/E)_0$ is the width for vanishingly small window, dE. The dE used here was 3 volts. The broadening of the distribution curves due to this window is negligible.

IV. RESULTS

A test run was made using a three-liter tank of toluene (15 cm diameter×20 cm deep). The more significant counting rates are listed in Table I. Figure 6 is a differential pulse-height distribution of $\mu\gamma$-β events; the energy calibrations are estimated from a Cs^{137} calibration. The distribution is roughly Gaussian with a peak at approximately 90 kev and a full width of 50%. This peak is to be attributed to the $2p-1s$ mesonic x-ray of carbon.

The 4-liter tank of dioxane (Fig. 1) was substituted for the toluene and the measurements were continued. The more important counting rates (for a portion of these measurements) are shown in Table II. Energy calibrations were performed periodically using the photopeaks of the 663-kev gamma ray of Cs^{137} and the 134- and 80-kev gamma radiation from Ce^{144}. The extrapolation from the higher energy gamma rays (i.e., the 663-kev gamma ray of Cs^{137}) was not suitable because of a nonlinearity in the response of the 6364 photomultiplier.[16]

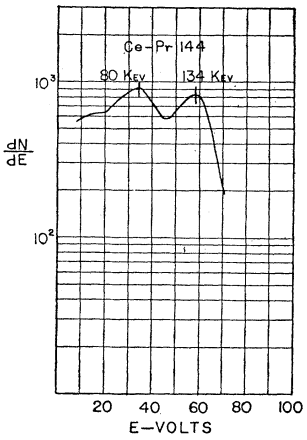

FIG. 5. Ce-Pr^{144} calibration curve. The ordinates are counts (per 10 seconds) for a 3-volt window; the abscissa is the pulse height in volts.

Figure 7 is the pulse-height distribution of 335 $\mu\gamma$-β (on scale) events.[17] The energies for carbon and oxygen are 83 kev and 146 kev. The full widths are 81% for the carbon peak and 53% for the oxygen peak. Some broadening of the carbon peak is anticipated because of Compton degradation of the oxygen $2p-1s$ peak. The suggestion of low-energy radiation at the lower edge

[16] Nonlinearity in a photomultiplier of similar construction has been reported [see R. W. Pringle and S. Standil, Phys. Rev. **80**, 762 (1950)]. S. Koslov (private communication) has observed that the combination of a NaI crystal used with a 5819 photomultiplier was linear over a wide range of energies, whereas the same NaI crystal with a type 6292 photomultiplier was nonlinear. In the present apparatus, using a NaI crystal and type 6364 photomultiplier, the calibration constant in kev/millivolt was 12% higher at 663 kev as compared to 134 kev. This nonlinearity may be related to the biasing of the photomultiplier shield element relative to the cathode and first dynode.

[17] Several different gain settings are represented in this distribution. The data have been corrected and plotted to the calibrated energy scale. The data listed in Tables II and III apply to a portion of these measurements at a given (constant) gain setting.

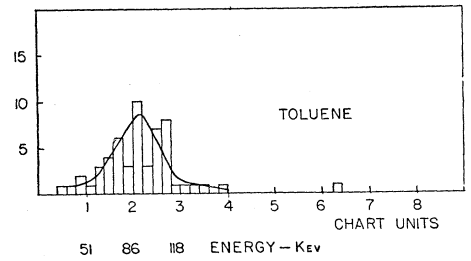

FIG. 6. Mesonic x-ray spectrum from carbon (toluene). The ordinate is the number of events per 0.2 chart division interval. The abscissa (upper number) is the chart division; the lower values are the corresponding energies in kev as estimated from a Cs^{137} calibration.

of the carbon peak is attributable to the combined effects of the oxygen $3d-2p$ radiation and the carbon $2p-1s$ escape peak.[18]

It is possible to extrapolate the carbon and oxygen curves to appropriate half-widths and to determine the areas under each curve. After corrections for detector efficiency and for the loss due to nuclear absorption, this procedure yields a ratio for captures on oxygen to those on carbon of 0.29 ± 0.04.

The time distribution of delayed coincidence μ-β events in toluene for the natural mixture of cosmic ray μ mesons is plotted in Fig. 8. A sufficient number of events are represented to yield a value of 2.13 ± 0.07 μsec for the mean life.[19] The time distribution of a portion of the $\mu\gamma$-β events in dioxane is listed in Table III and also plotted in Fig. 8 superimposed on a 2.13 μsec decay curve. The mean life of the negative μ mesons in oxygen is 1.9 μsec[20] (as compared to 2.0 μsec in carbon[21]). However, the diluting effect of the off-scale $\mu\gamma$-β events[22] would be expected to nullify the significance

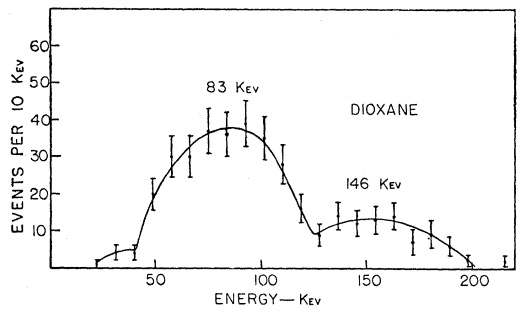

FIG. 7. Mesonic x-ray spectrum from carbon and oxygen (dioxane). The ordinate is the number of events per 10-kev energy interval; the abscissa is the energy as estimated from a $Ce\text{-}Pr^{144}$ calibration.

[18] In the measurement of low-energy gamma radiation by NaI, the photoelectric peak is usually accompanied by a subsidiary peak (escape peak) lying below the main peak by the K shell binding energy of iodine (33 kev). This is due to events in which the iodine x-ray resulting from the photoelectric effect is not absorbed in the crystal.

[19] A. Fafarman and M. H. Shamos, Phys. Rev. **96**, 1096 (1954).

[20] H. K. Ticho, Phys. Rev. **74**, 1343 (1948).

[21] H. A. Morewitz and M. H. Shamos, Phys. Rev. **92**, 134 (1953).

[22] These usually correspond to the stopping of positive μ mesons n the NaI crystal.

TABLE I. Toluene (3-liter tank).

Running time	138 hr
$\mu\gamma$-β events (101, 40, 16, 4)	161
$\mu\gamma$-β events (on-scale; <370 kev)	54
$\mu\gamma$-β rate	1.20±0.09/hr
μ-β rate	12±2/hr
$\mu\gamma$ rate	64/min

of the slightly shortened mean life in oxygen on the delay distribution of the $\mu\gamma$-β events in dioxane.[23]

V. POSSIBLE SOURCES OF ERROR

A. Energy Measurement

The energy resolution at this energy (100 kev) is only ~40%.[24] Periodic energy calibrations showed an average deviation of ±2%.[25] The low resolution, together with the statistical uncertainties, makes it difficult to determine the position of the photoelectric peaks for the experimental curves. The calibrations showed the type 6364 photomultiplier to be nonlinear; the ratio of the calibration constants (kev/millivolt) at 660 kev and at 100 kev was 1.14±0.02. There is a small error attributable to the nonzero slope or irregularity of the stretched pulse.[26] The maximum correction for this is −2%. The pulse lengthener baseline showed a slight dependence on the counting rate which was less than 2% of full scale. The data in Fig 7 have been corrected for the nonlinearity of the photomultiplier and for the nonzero slope of the stretched γ pulse.

B. Accidental and Other Events

From the values in Table III, the calculated $N_{\mu\gamma}$ (accidental) = 0.008/min, which is negligible in relation to the $\mu\gamma$ rate of 76/min.

However, $N_{\mu\gamma\text{-}\beta}$ (accidental) = 0.17/hr. This is 10% of the observed rate; since the usual $\mu\gamma$ event is a meson passing completely through the NaI crystal, these accidentals will be off-scale events of several Mev.

TABLE II. Dioxane (4-liter tank).

Running time	266 hr
$\mu\gamma$-β events	401
$\mu\gamma$-β events (on-scale; <250 kev)	142
$\mu\gamma$-β rate	1.51+0.08/hr
μ-β rate	20±6/hr
$\mu\gamma$ rate	76/min

[23] In addition roughly twice as many captures of negative μ mesons occur on the carbon as on the oxygen. However, the predominant contribution is that of the off-scale events.

[24] Although better resolution would have been obtained with a smaller detector, a large area detector was chosen because of the low intensity of events.

[25] Based on the internal consistency of the various calibrations (i.e., no allowance is made for possible systematic errors).

[26] This refers to the γ pulse which is stretched from a duration of 4 μsec to one of 20 μsec whenever a $\mu\gamma$ coincidence occurs.

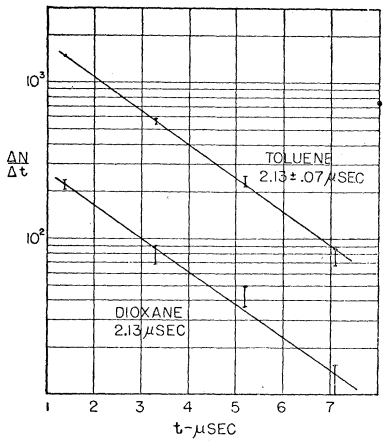

FIG. 8. Differential delay distributions for toluene and dioxane. The ordinate is the differential channel count, the abscissa the delay in μsec.

The above accidentals are attributable to random coincidences. However, the largest component of the $\mu\gamma$-β rate is due to positive mesons passing through the tank which stop and decay in the NaI crystal. Estimating the probability for the decay positron to pass through the tank giving an apparent $\mu\gamma$-β event, leads to a calculated rate which is 2 to 3 times as great as the calculated rate for the events under study; this calculation is in good accord with the experimental data (Table II); such events corresponding to the stopping and decay of positive mesons in the NaI crystal will, of course, be very energetic and off-scale (>10 Mev).

C. Capture Ratio

The experimental value for the ratio of captures in mesonic atom formation by oxygen and carbon was computed by two methods:

(a) measurement of the areas under the carbon and oxygen peaks.

(b) comparison of the peak values.

After correction for the detection efficiency and for the loss due to nuclear absorption, values of 0.29±0.04 and 0.36±0.04 were obtained. These values are in error because of Compton degradation of the oxygen $2p-1s$ radiation in the tank (~14 cm depth) and the escape peak (in the NaI crystal) of the oxygen $2p-1s$ radiation; both of these effects appear under the carbon peak. The expected result is a broadening of the carbon peak and this is in fact observed.

VI. DISCUSSION

An approximate calculation based on the known rate of meson stoppings in the tank and on the computed detection efficiency, indicates that almost every stopping meson makes a radiative transition to the ground ($1s$) state of a carbon or of an oxygen mesonic atom. The energy resolution is not sufficient to distinguish the presence of a small admixture of higher orbital transitions (e.g., $3p-1s$) in addition to the $2p-1s$ radiation.[27] However, the discrepancy between the measured energies and the computed values (Appendix I) for the $2p-1s$ carbon and oxygen mesonic x-rays, while not outside the experimental errors, indicate the presence of some transitions with $n>2$ to $n=1$.

TABLE III. Counting rates—dioxane.

Hours	$\mu\gamma$ Rate	Channel 1	2	3	4	$\mu\gamma$-β Total	On-scale	$\mu\gamma$-β Total rate
18.7	74/min	18	4	4	1	27	7	1.4 ±0.3/hr
91.4	74	62	28	16	5	111	40	1.21±0.12
85.1	77	86	27	13	13	139	48	1.63±0.14
70.4	77	67	30	22	5	124	47	1.76±0.16
Totals 265.6		233	89	55	24	401	142	1.51±0.08
								on-scale 0.53±0.05
Totals corrected[a]		221	77	43	12			

[a] Corrected for accidental counts 0.044/hr in each channel.

The validity of the Z-dependence law for the probability of forming mesonic atoms on the various elements of a chemical compound remains obscure. The results in this experiment are vitiated partly because of the incomplete resolution of the carbon and oxygen curves, and because of Compton degradation of the energy of the oxygen mesonic x-ray, which shifts oxygen events to the carbon peak.[28] The surmounting of these difficulties involves the use of a thin dioxane absorber as opposed to the thick dioxane absorber used in the present experiment. The use of a thin absorber virtually rules out cosmic ray mesons as the source; however, an artificial μ-meson beam should be suitable, provided that a delayed coincidence method is used to eliminate the low-energy background radiation often present in accelerator experiments.

VII. ACKNOWLEDGMENTS

We wish to thank Dr. L. Spruch for several helpful suggestions during the course of this work.

APPENDIX I. MESONIC X-RAYS ENERGIES IN CARBON AND OXYGEN

The energy levels of the mesonic carbon and oxygen atoms can be computed from the point nucleus (hydrogen-like) solutions of the Schrödinger equation. The solutions (energy eigenvalues) for this equation are:

$$E_n=-\tfrac{1}{2}\mu c^2(\alpha Z/n)^2,$$

[27] This admixture should be small because of the greater statistical weight of the circular orbits, $\ell=n-1$, in the meson capture process. See G. R. Burbridge and A. H. DeBorde, Phys. Rev. 89, 189 (1953).

[28] *Note added in proof.*—To check the effect of the Compton scattering, a separate calibration has been performed using a "phantom," i.e., a container of water geometrically similar to the dioxane tank and having a weak Ce-Pr^{144} source dispersed uniformly throughout. The observed spectrum did not differ markedly from that obtained with the bulk source; an upper limit of about 10% could be set on events lost from the 134-kev peak to lower energies. Hence it does not appear that Compton degradation of the oxygen $2p-1s$ radiation is responsible for the discrepancy.

where μ is the reduced mass of the meson, α the fine structure constant, Z the atomic number, and n the principal quantum number.

The solution for the finite nuclear radius (nonpoint source) is obtained by a first-order perturbation calculation using the potential.[29]

$$V(r)=-(Ze^2/R)(\tfrac{3}{2}-\tfrac{1}{2}r^2/R^2) \quad \text{for} \quad r\leq R$$
$$=-Ze^2/r \quad \text{for} \quad r\geq R,$$

where $R=1.2\times10^{-13}A^{\frac{1}{3}}$ cm (nuclear radius).

It suffices for low-Z materials to calculate the perturbation of the $1s$ level. The higher levels $n\geq 2$, except in the heaviest elements, satisfy the point nucleus solutions. The fractional energy shift due to the perturbation is[30]

$$\Delta E/E_{1s}=-\tfrac{4}{5}Z^2(R/a_0)^2,$$

where $a_0=\hbar^2/\mu e^2=2.52\times10^{-11}$ cm (radius of the first Bohr orbit of the mesonic hydrogen atom).

The K and L shell energies obtained from the point nucleus solutions of the Schrödinger and the Dirac[31] wave equations are shown in Table IV. The perturbation correction has been applied to the $1s$ level.

TABLE IV. μ-mesonic atoms—lowest energy levels (in Mev).

Z	$1s_{\frac{1}{2}}$	$2p_{\frac{1}{2}}$	$2p_{\frac{1}{2}}$ $2s_{\frac{1}{2}}$	$2p_{\frac{3}{2}}-1s_{\frac{1}{2}}$	Computed from
6	−0.1018	−0.0254	⟶	0.0764	Schrödinger
	−0.1019	−0.0254	($2p_{\frac{3}{2}}$ −12 kev)	0.0765	Dirac
	−0.1015			0.0761	Perturbation of Dirac solution
8	−0.1823	−0.0456	⟶	0.1367	Schrödinger
	−0.1824	−0.0456	($2p_{\frac{3}{2}}$ −47 kev)	0.1368	Dirac
	−0.1807			0.1351	Perturbation of Dirac solution

[29] See reference 6, footnote on p. 173.

[30] This result is obtained also by L. N. Cooper and E. M. Henley, Phys. Rev. **92**, 801 (1953), their Eq. (11).

[31] $E_{n,j}=\mu c^2\left[1+\dfrac{(\alpha Z)^2}{\{n-|k|-(k^2-\alpha^2Z^2)^{\frac{1}{2}}\}^2}\right]^{-\frac{1}{2}}$
$\cong\mu c^2\left[1-\dfrac{(\alpha Z)^2}{2n^2}-\dfrac{(\alpha Z)^4}{2n^4}\left(\dfrac{n}{|k|}-\dfrac{3}{4}\right)\right]$, $k=-\ell-1$ for $j=\ell+\frac{1}{2}$, $k=\ell$ for $j=\ell-\frac{1}{2}$.

PHYSICAL REVIEW VOLUME 100, NUMBER 3 NOVEMBER 1, 1955

Angular Correlation Effects in V-Particle Decay

S. B. TREIMAN AND H. W. WYLD, JR.
Palmer Physical Laboratory, Princeton University, Princeton, New Jersey

(Received June 6; revised manuscript received September 16, 1955)

In decay processes of the types: hyperon→nucleon+pion; or K-meson→pion+pion, the most general distribution function in η—the angle between the decay plane normal and a reference direction **N** normal to the line of flight of the unstable particle—has the form of a finite Fourier series. The degree of the highest harmonic is simply related to the spin of the unstable particle. The coefficients in the series depend on the state of polarization of the spin with respect to the reference direction **N**. It is possible however to set upper limits on the coefficients; this may prove useful in any attempt to analyze angular correlation data, particularly in the case of hyperon decay. The upper limits for various low spin values are computed, and other consequences of the angular momentum and parity conservation laws are discussed.

I. INTRODUCTION

ANGULAR correlation effects in V-particle decay have been investigated recently by a number of workers,[1–5] in an attempt to learn something about the spins of the new unstable particles. For reasons of parity and angular momentum conservation, a particle of spin zero or spin one-half must decay isotropically in its rest frame. In the case of particles which undergo two-body decay, this means that the distribution in η—the angle between the decay plane normal **n** and any reference direction **N** which is normal to the line of flight of the unstable particle and which is defined independently of **n**—must be uniform.[6] A nonuniform distribution in η would automatically imply spin greater than one-half; and from the form of the distribution (see below) one could set a lower limit to the value of the spin.

Even for particles of very large spin, however, angular correlation effects would show up only if the spins were somehow polarized (i.e., nonrandomly distributed) with respect to the reference direction **N**. This suggests that the effect, if it exists at all, would be most likely to manifest itself with unstable particles produced in low-energy interactions of elementary particles, e.g., the reaction $\pi^-+p\rightarrow$hyperon+K-meson observed at Brookhaven. Nevertheless, early Princeton work[1] on V^0-particles produced in generally complex

[1] Ballam, Hodson, Martin, Rau, Reynolds, and Treiman, Phys. Rev. **97**, 245 (1955); see also *Proceedings of the Fifth Annual Rochester Conference on High-Energy Physics* (Interscience Publishers, Inc., New York, 1955).

[2] Report by C. D. Anderson, *Proceedings of the Fifth Annual Rochester Conference on High-Energy Physics* (Interscience Publishers, Inc., New York, 1955).

[3] G. D. James and R. A. Salmeron, Phil. Mag. **46**, 571 (1955).

[4] Sreekantan, Pevsner, and Sandri, Phys. Rev. **98**, 642 (*A*) (1955).

[5] Fowler, Shutt, Thorndike, and Whittemore, Phys. Rev. **98**, 121 (1955).

[6] Treiman, Reynolds, and Hodson, Phys. Rev. **97**, 244 (1955).